UNIVERSITY OF LEEDS

Investigating metabolic reprogramming by GR and LXR in triple negative breast cancer

MRes Medicine

School of Medicine University of Leeds

By

Anna Nicholls

Supervised by Dr Laura Matthews, University Academic Fellow, School of Medicine, University of Leeds, and Dr James Thorne, School of Food Science and Nutrition, University of Leeds

July 2020

Thank you to the Pathological Society and the Wolfson Foundation for their generous sponsorship of this project

and the help of Freya Leif, Fiona Leslie, and Kathryn McGinnis in the laboratory

Pathological Society of Great Britain & Ireland Understanding disease

The Wolfson Foundation

Due to the COVID-19 pandemic the lab work for this project finished prematurely. As a consequence, different experiments had been started to work towards the project aims but no experiment had sufficient experimental repeats for statistical analysis. After discussion with The Pathological Society it was decided that this report would be written in a way that explains what I have done this year but also my experience of the course and research during the lockdown period. I hope that this report and the lessons I learnt which I have shared may be useful to future students considering pathology research as part of their intercalated degree.

Contents

Introduction……………………………………………………………………………..4
Hypothesis………………………….……………………………………………………..7
Specific aims…………………………..……………………………………………………...7
Does OCDO induce GR nuclear translocation? …………………………………………7
Does OCDO activate GR and LXR to drive transcription? ……………………………11
What endogenous genes to GR and LXR coregulate?…………………………………14
Discussion…………………………..……………………………………………………….20
A COVID-affected course experience..…………………………………………………21
Acknowledgements...………………………………………………………………...22
References...……………………………………………………………...............22
Appendix...………………………………………………………….................25

Introduction

Breast cancer (BC) affects one in seven women in their lifetime (1). BCs are subtyped according to the expression of three receptors. These subtypes are used to stratify treatment (2). Tumours expressing the oestrogen or progesterone receptors are treated with Tamoxifen or aromatase inhibitors. Tumours expressing the Human epidermal growth factor receptor (HER2) are treated with Herceptin, a HER2 inhibitor (3).

Triple negative breast cancer (TNBC) is an additional BC subtype which lacks expression of these receptors. TNBC is aggressive and accounts for 15-20% of BCs. Only the 10-15% of TNBC patients who have the *BRCA1* or *BRCA2* mutations may benefit from Poly (ADP-Ribose) Polymerase inhibitors. For the remaining patients no targeted treatments are available for early stage disease (4). Despite chemotherapy, residual disease remains for 60-80% of patients and these patients have a poor prognosis (5,6). A new treatment is urgently needed.

The oestrogen and progesterone receptors are nuclear receptors (NR). NRs are ligand-activated transcription factors. Activation by a specific ligand results in regulation of expression of specific genes involved in cell fate, immunity, and metabolism (7,8). There are two main types of response mediated by NRs; Type I NRs translocate into the nucleus upon ligand binding whilst Type II NRs are constitutively bound to DNA but are only active upon ligand binding (Figure 1) (9,10). Nuclear receptors are highly druggable targets. Analysis of differentially expressed NRs in TNBC identified a strong metabolic signature (Figure 2) (Pfaender, unpublished). Within this signature, the glucocorticoid receptor (GR) and the Liver X Receptor (LXR) were differentially expressed suggesting that GR and LXR are potential drug targets for TNBC. Previously, high expression of GR showed association with worse prognosis in TNBC and antagonism of GR has shown some promise in early stage trials (11–13).

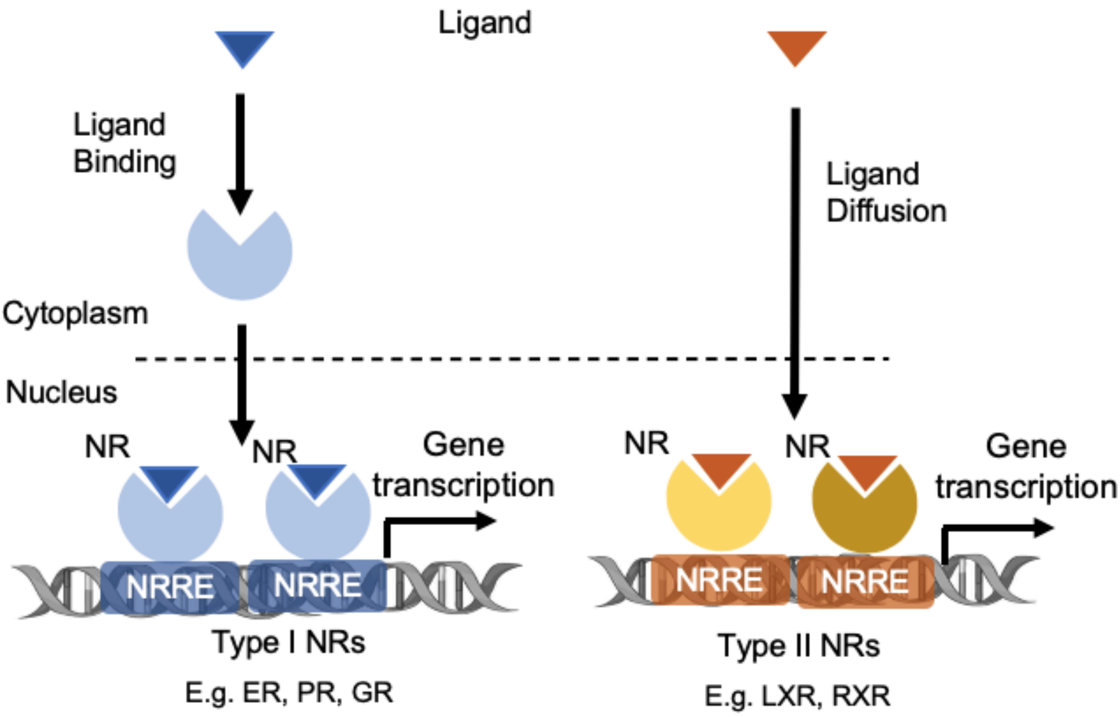

Figure 1: Two models of nuclear receptor (NR) action. Left: Type I NRs such as the oestrogen receptor (ER), progesterone receptor (PR) and the glucocorticoid receptor (GR) reside in the cytoplasm when they are not bound to a ligand. Upon ligand binding, the ligand-receptor complex translocates into the nucleus, binds to DNA at the nuclear receptor response element (NRRE) and recruits coregulators (CoReg) to activate or inhibit gene transcription. Right: Type II NRs such as Liver X receptor (LXR) and Retinoid R receptor (RXR) are constitutively nuclear even when inactive, and bound directly to DNA. Figure was created from results described in (9) and (14).

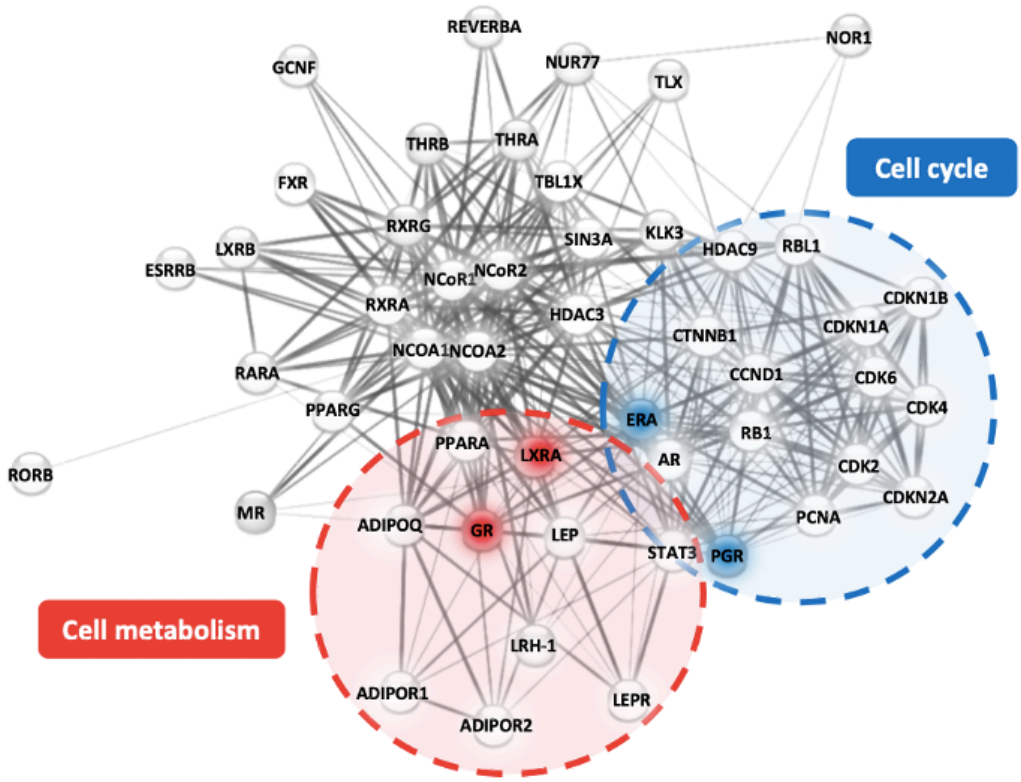

Figure 2: Bioinformatic analysis of nuclear receptor networks in BC. String analysis of differentially expressed nuclear receptors was completed, and an additional two interactome layers included to predict protein interaction networks. A cell cycle network emerges for tumours containing Oestrogen (ER) and Progesterone (PGR) receptors (blue circle) whereas a cell metabolism network emerges for TNBC tumours that contain Glucocorticoid (GR) and Liver X (LXR) receptors (red circle). Profiling of nuclear receptor expression, the string analysis and the production of this Figure was completed by Pauline Pfaender, as part of an Erasmus project (Pfaender, unpublished).

Furthermore, a cholesterol-derived oncometabolite, 6-oxo-cholestan-3β,5α-diol (OCDO), is present at higher levels in TNBC tissue compared to normal breast tissue and high levels of OCDO are associated with worse prognosis (15). The endogenous GR and LXR ligands (cortisol and 27-hydroxcholesterol) are also cholesterol-derived. OCDO drives GR-dependent proliferation and has been shown to bind to LXR however the role of OCDO in relation to lipid metabolism remains unexplored (15).

Hypothesis

OCDO promotes GR and LXR activation and crosstalk in breast and promotes detrimental cell metabolism in TNBC. Modulation of GR and LXR activity/crosstalk may restore normal cell metabolism and therefore offer therapeutic benefit.

Specific aims

1. Determine the effect of OCDO on GR nuclear translocation, a marker of activation.
2. Establish if OCDO can activate GR and LXR to drive transcription of reporter genes containing consensus response elements.
3. Use existing data and bioinformatic tools to predict potential pathways and genes that are commonly regulated by GR and LXR cross-talk.

Two further aims if the pandemic had not occurred were:

1. Confirm GR and LXR regulation of a small panel of genes.
2. Assess the outcome of using GR and LXR modulators on coregulated pathways.

Does OCDO induce GR nuclear translocation?

To determine the effect of OCDO on GR nuclear translocation MDA-MB-231 and MDA-MB-468 TNBC cells were treated with 100nM Dexamethasone (a positive control) or 10μM OCDO for 1, 4, and 24 hours. Cells were fixed and stained for GR, the nucleus and the actin cytoskeleton. Cytoplasmic and nuclear GR were imaged, quantified and the nuclear GR: cytoplasmic GR ratio determined using ImageJ and Cell Profiler. Two different microscopes were used to optimise the imaging process. A pipeline was produced using Cell Profiler which reliably identified nuclei and cytoplasm in the EVOS microscope images but this was not possible for the Widefield microscope images despite trying multiple different methods to identify cytoplasm outlines. Consequently only EVOS microscope images were used. This experience provided an opportunity to work through a computer-based problem systematically and judge when it is appropriate to continue with an issue and when to accept it is not working and move on.

For all time points Dexamethasone induced GR translocation in the nucleus in both cell lines compared to untreated cells. OCDO appeared to induce some GR translocation in MDA-MB-231 but not MDA-MB-468 cells, which was more evident at higher magnification (Figures 3-4, expanded fields Appendix Figures A-D). LXR is constitutively bound to DNA so activation by OCDO could not be assessed using immunofluorescence.

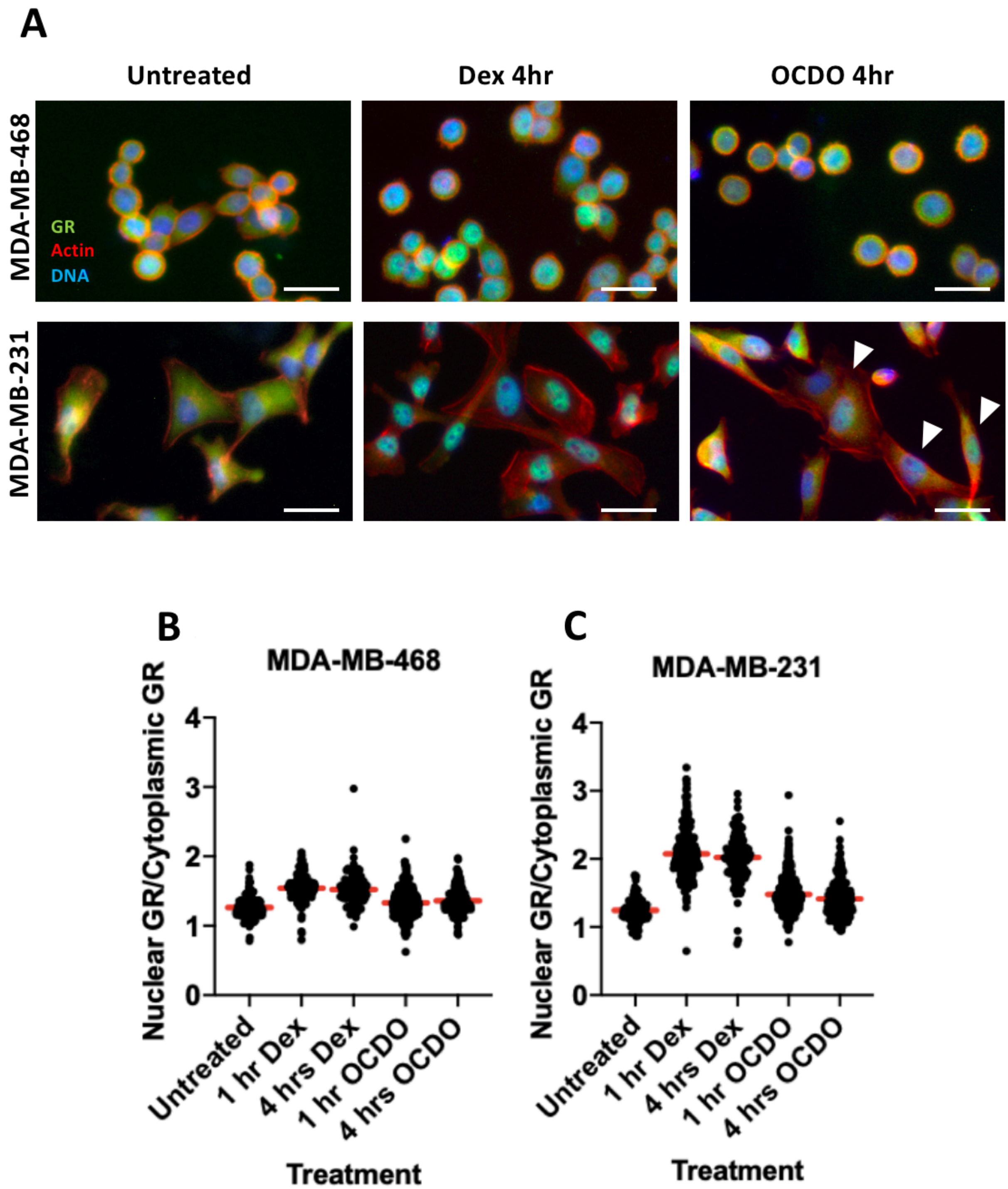

Figure 3: Quantification of ligand induced nuclear GR translocation in MDA-MB-468 and MDA-MB-231 cells after 1 and 4 hours. (A) Higher magnification images from Appendix figures A and B. As indicated, green GR, red actin and blue DNA. White arrowheads highlights OCDO treated cells with nuclear GR. Scale bar, 10μm. (B and C) Scatterplots showing nuclear/cytoplasmic ratios of GR after 1 and 4 hour treatments with 100nM Dexamethasone (Dex) or 10μM OCDO in MDA-MB-468 and MDA-MB-231 cells, quantified using cell profiler. Higher values indicate more nuclear GR. Red bars show mean ratio. N=1.

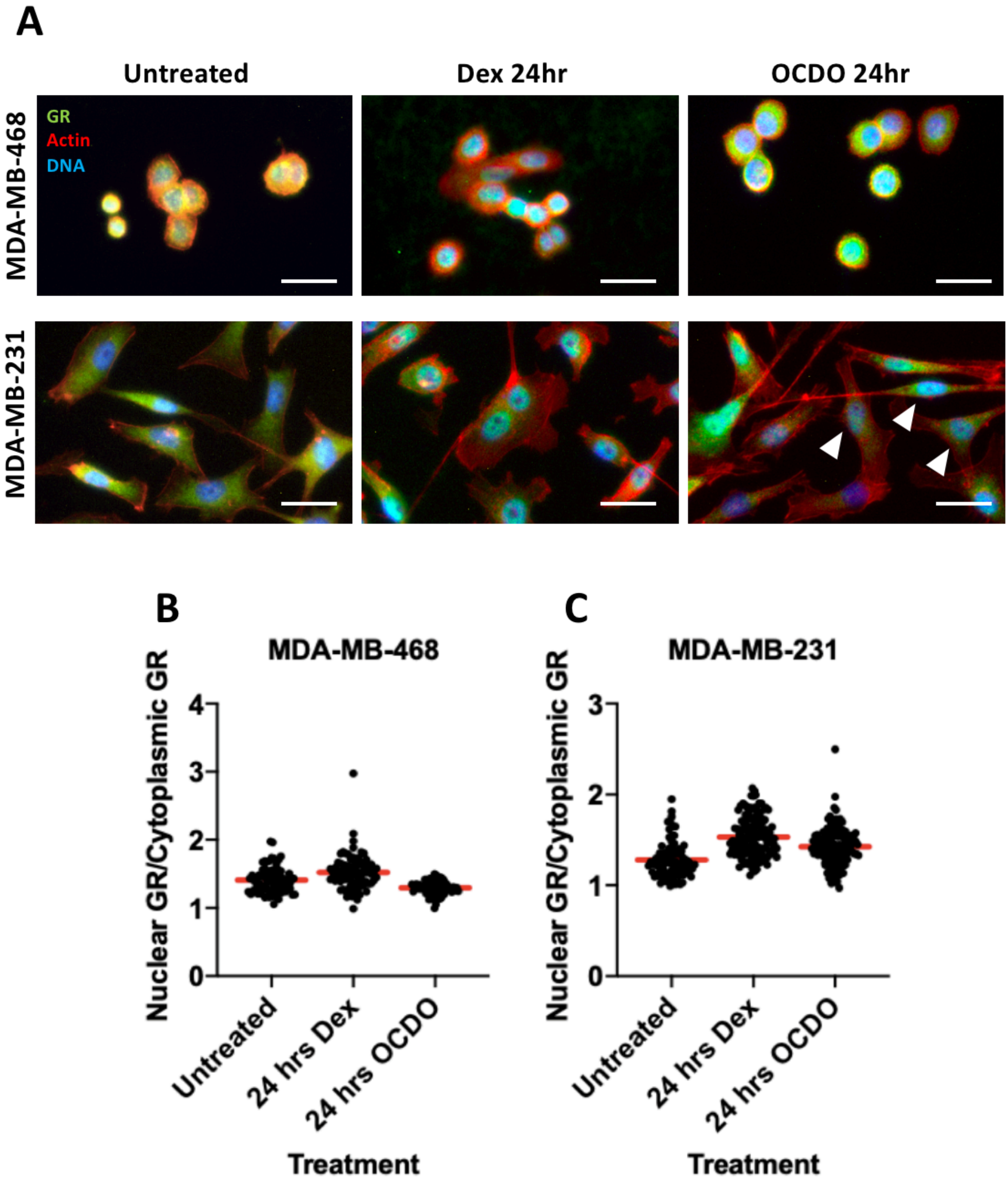

Figure 4: Quantification of ligand induced nuclear GR translocation in MDA-MB-468 and MDA-MB-231 cells after 24 hours. (A) Higher magnification images from appendix figures C and D. As indicated, green GR, red actin and blue DNA. White arrowheads highlights OCDO treated cells with nuclear GR. Scale bar, 10µm. (B and C) Scatterplots showing nuclear/cytoplasmic ratios of GR after 24 hours treatments with 100nM Dexamethasone (Dex) or 10µM OCDO in MDA-MB-468 and MDA-MB-231 cells, quantified using cell profiler. Higher values indicate more nuclear GR. Red bars show mean ratio. N=1.

Does OCDO activate GR and LXR to drive transcription?

A reporter gene assay (a synthetic system designed to measure transcription factor activity) was used to investigate transcription. MDA-MB-231 and MDA-MB-468 cells were transfected with a specific response element that drives luciferase enzyme expression fused to the promoter region of a GR or LXR target gene (*TAT3* and *ABCA1* respectively). When the transfected cells are treated with a drug targeting the transcription factor that regulates that gene's expression and luciferin substrate is added, light is produced (Figure 5). A luminometer measures the light output; the more light there is the more transcription factor activation there is. Cells were treated with OCDO and two positive controls, Dexamethasone and GW3965 (known GR and LXR agonists respectively).

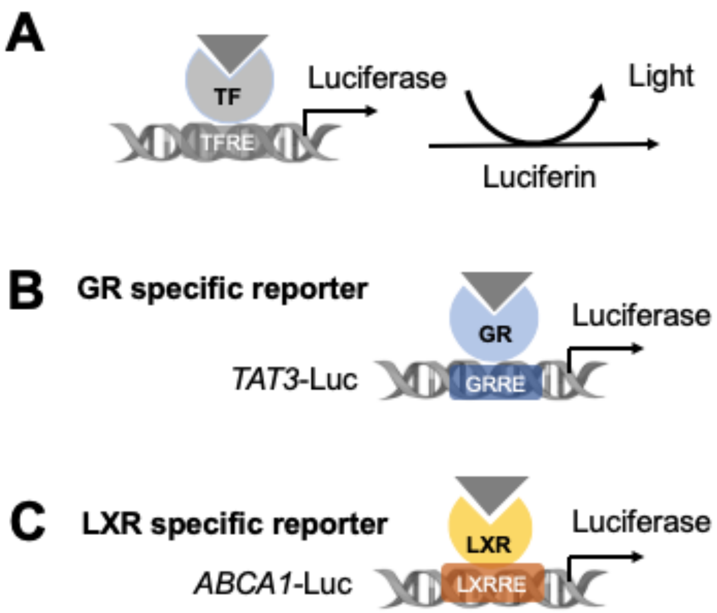

Figure 5: Diagrammatic representation of the GR and LXR reporters. (A) Transcription factor (TF) binding to the transcription factor response element (TFRE) activates luciferase production. When luciferin substrate is added light is produced. (B) The glucocorticoid receptor (GR) specific reporter which works as described in (A). Activation of the GR promoter of the *TAT3* gene results in light production. (C) The Liver X Receptor (LXR) specific reporter which works as described in (A). Activation of the LXR promoter of the *ABCA1* gene results in light production. *TAT3*-Luc was a generous gift from Dr J Iniguez-Lluhi (16). *ABCA1*-Luc was purchased from Addgene (#86442 (17)).

Dexamethasone-treated cells showed a dose response for both cell lines transfected with the GR reporter. In MDA-MB-468 and MDA-MB-231 cells the mean luciferase activity increased modestly as OCDO concentration reached 3μM (Figure 6). The response to OCDO was not as potent as Dexamethasone, indicated by the response to significantly lower concentrations of Dexamethasone compared to OCDO.

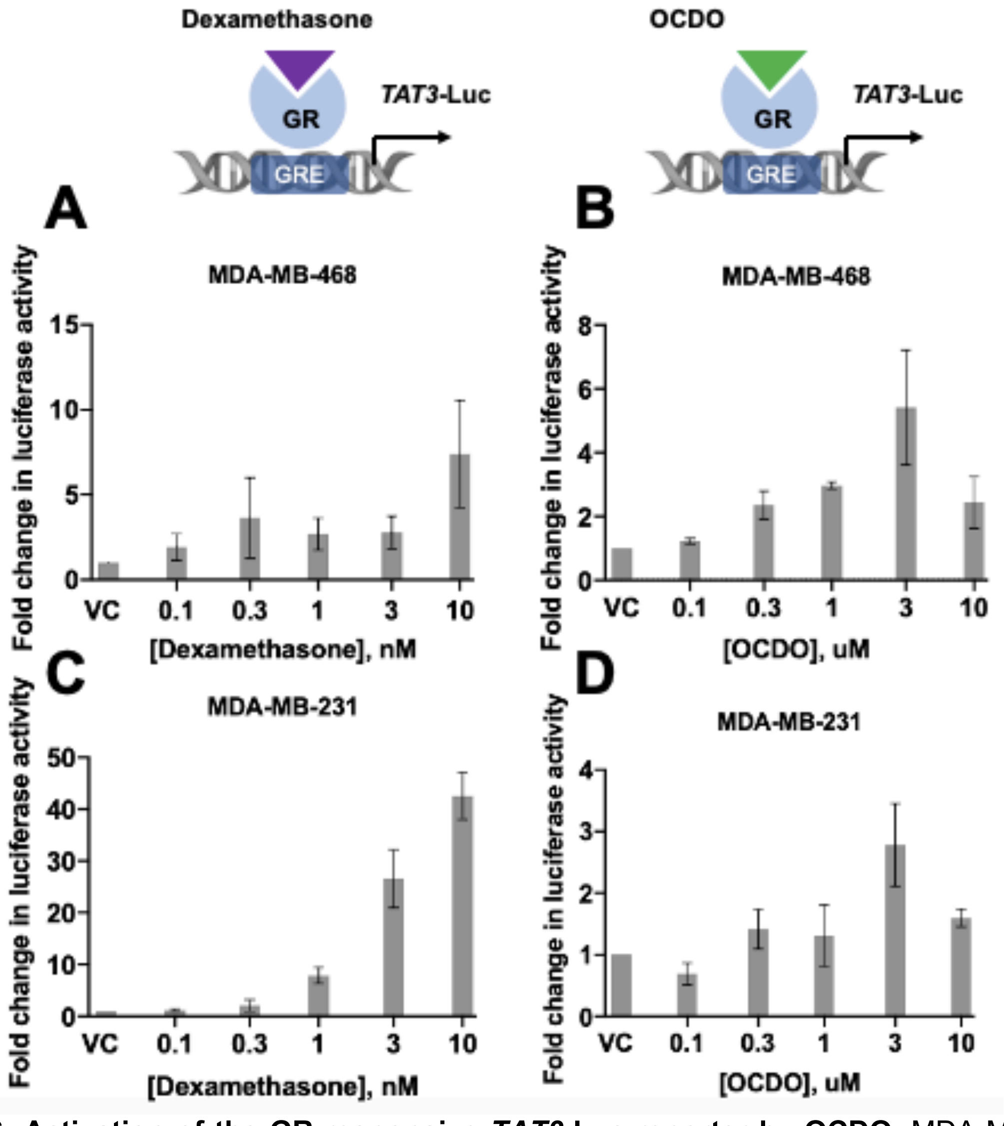

Figure 6: Activation of the GR responsive *TAT3*-Luc reporter by OCDO. MDA-MB-468 and MDA-MB-231 cells were transfected with a *TAT3*-Luc reporter plasmid then treated with serial dilutions of Dexamethasone or OCDO in charcoal stripped calf serum for 16 hours. Fold change in luciferase activity relative to luciferase activity in DMSO vehicle control treated cells. Error bars show standard error of the mean (A and B) and standard deviations from technical replicates (C and D). (A and B) n=2. (C and D) N=1.

These preliminary data suggest that OCDO causes GR to translocate into the nucleus in MDA-MB-231 cells but possibly not in MDA-MB-468 cells. However, OCDO mediated GR-regulated transcription in both cells lines. Insufficient numbers of repeats were completed for the immunofluorescence and luciferase assays due to limited time and hence no statistical analysis could be performed. Thus the hypothesis that Dexamethasone and OCDO cause GR translocation into the nucleus cannot be accepted nor rejected. The data so far is promising however in supporting the hypothesis.

MDA-MB-231 and MDA-MB-468 cells transfected with the LXR reporter showed dose responses for GW3965 and OCDO (Figure 7). Thus the preliminary results suggest that OCDO can activate GR- and LXR-mediated transcription in MDA-MB-468 and MDA-MB-231 cells although there was a greater response to LXR in MDA-MB-231 cells than MDA-MB-468 cells.

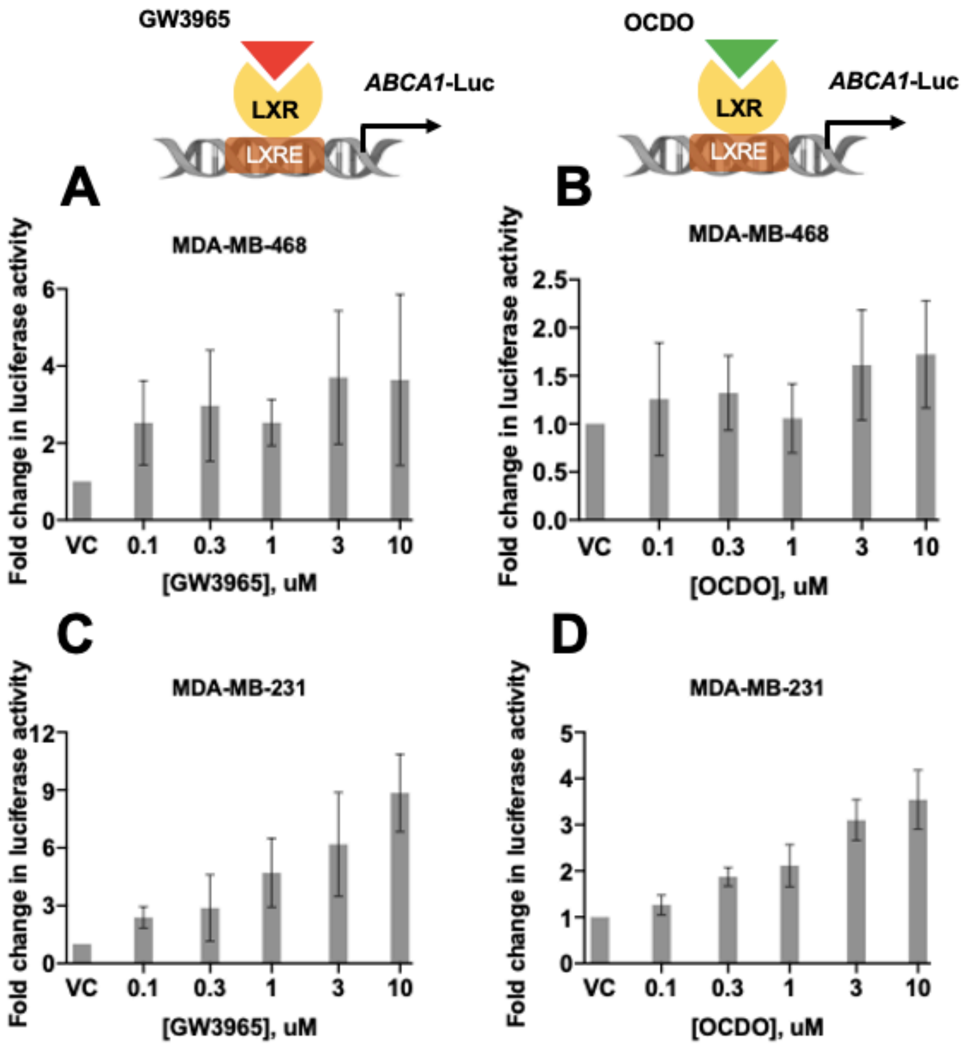

Figure 7: Activation of the LXR responsive *ABCA1*-Luc reporter by OCDO. MDA-MB-468 and MDA-MB-231 cells were transfected with an *ABCA1*-Luc reporter plasmid and treated with serial dilutions of GW3965 and OCDO in charcoal stripped serum for 16 hours. Fold change in luciferase activity relative to luciferase activity in DMSO vehicle control treated cells. Error bars show standard error of the mean for N=2 (A and B) and standard deviation of three technical repeats (C and D). (A and B) n=2. (C and D) N=1.

What endogenous genes to GR and LXR coregulate?

To identify genes that OCDO may have an effect on via GR- and LXR-mediated transcription, available online Chromatin Immunoprecipitation-sequencing (ChIP-seq) datasets for GR and LXR were quality assessed during the lockdown period. Ideally we would have done ChIP-seq on our cells and the second best option would have been comparing datasets for GR and LXR in human breast. However, research on LXR is in its infancy so limited datasets were available. Other datasets had to be analysed to select the best possible comparison (Table 1). For me, this was an insight into potential limitations within research and how science can't always use the gold-standard methods but other methods may be available that, although aren't ideal on their own, when used together they are a useful substitute. In this project that meant identifying possible important genes in TNBC coregulated by GR and LXR and confirming their regulation using PCR.

No direct human tissue comparisons could be made because of poor quality datasets for either GR or LXR for any given available tissue (Table 1). As mouse datasets are commonly used to predict responses in humans, NR binding data in same tissue mouse datasets were considered as a possible proxy. However, when these were overlaid with GR in human normal and TNBC breast tissue there was negligible overlap possibly due to the complexity of human breast tissue and 5000 gene targets being too restrictive (Figure 8). Increasing the number of gene targets selected above 5000 was an option but this risked including more constitutively activated genes that are not important to TNBC pathology. Therefore, it was next considered whether GR in human breast could be compared with LXR in another human tissue. The best comparison was between GR in normal and TNBC breast and LXRα in human adipose tissue which showed 243 genes coregulated by GR and LXRα specific to TNBC (Figure 9).

Table 1: List of available human LXRα, LXRβ, and corresponding GR gene target datasets available for analysis from the Cistrome database (18,19)**.** A dash indicates that no datasets were available. Cistrome database ID, dataset reference.

Tissue	**Species**	**LXRα** Quality, Cistrome ID (ref)	**LXRβ** Quality, Cistrome ID (ref)	**GR** Quality, Cistrome ID (ref)
Breast (normal and TNBC)	Human	-	-	Normal – good 87683, (20) TNBC – moderate 56103, (21)
Colorectal adenocarcinoma	Human	Good 69800, (22)	Good 69805, (23)	Poor 38651, (24)
Monocytes	Human	-	Poor 8397, (25)	Good 50246, (26)
Adipose	Human	Good 41168, (27)	-	-
Macrophage	Mouse	Good 72544, (28)	Good 2645, (29)	Good 82532, (30)
Hepatocyte	Mouse	-	Good 5416, (31)	Good 37598, (32)

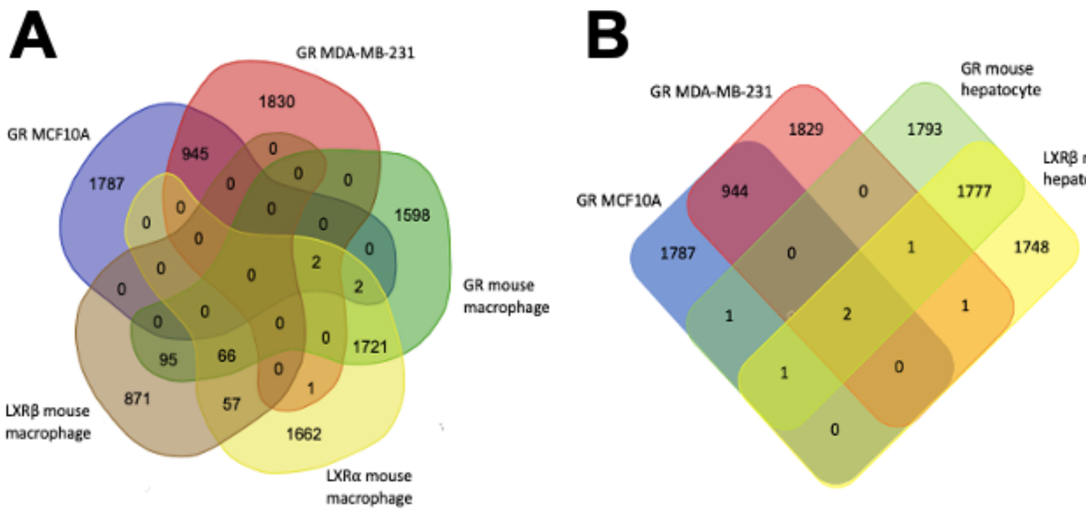

Figure: 8: Overlay of human and mouse ChIP-seq data for GR and LXRs. Publicly available ChIP-seq data for GR, LXRα and LXRβ were analysed using the Cistrome database. For each dataset, the top 5000 peaks annotated to genes (note some genes had multiple peaks) were selected and then compared using BioVenn (33). (A) Shows overlap between glucocorticoid receptor (GR) in normal human breast (MCF10A), human TNBC (MDA-MB-231), and mouse macrophages and for the Liver X Receptor (LXRα and LXRβ) in mouse macrophages. (B) Shows overlap between GR binding sites in normal human breast, human TNBC, and mouse hepatocytes and LXRβ binding sites mouse hepatocytes. Numbers represent the number of gene targets (not the number of peaks). Details of datasets are presented in Table 1.

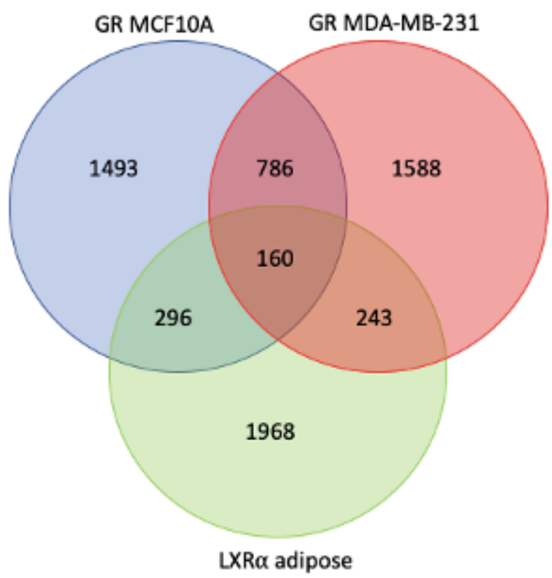

Figure 9: Overlay of human ChIP-seq data for GR and LXRs. Publicly available ChIP-seq data for GR, LXRα and LXRβ were analysed using the Cistrome database. For each dataset, the top 5000 peaks annotated to genes (note some genes had multiple peaks) were selected and then compared using BioVenn (33). Figure shows overlap between GR binding sites in normal human breast (MCF10A), human TNBC (MDA-MB-231), and LXRα binding sites in human adipose tissue. Numbers represent the number of gene targets (not the number of peaks). Details of datasets are presented in Table 1 .

Unbiased gene pathway analysis of those 243 genes using Enrichr (34,35) identified that lipid metabolism is likely to be an important point of GR and LXR crosstalk, which was consistent with the literature that outlines both NRs' functions independently (Figure 10). To test that this was not just a result of using an adipose dataset the analysis was repeated using LXRα and LXRβ in colorectal adenocarcinoma instead of adipose and enrichment of fatty acid biosynthesis remained (not shown). Next, genes involved in these pathways were identified. Five lipid genes (*FASN*, *ACACA*, *ADIPOR2*, *PRKAB1*, and *ABCA1)* were consistently enriched in these pathways but these genes could be regulated in different ways (Figure 11). NR binding graphs were used to identify genes bound by GR and LXR in common sites (36). *ABCA1* was excluded from further analysis as PCR analysis completed in the project but not discussed in this report suggested OCDO did not activate *ABCA1* transcription. While the *ACACA* gene had binding sites for GR, LXRα and LXRβ, there were no clear regions where binding sites were aligned (Figure 12A) suggesting GR and LXR may regulate *ACACA* independently. Meanwhile binding sites were more closely aligned for ADIPOR2, FASN, and PRKAB1 suggesting they GR and LXR may regulate these genes by crosstalk (Figure 12B-D). Therefore, these genes would have been taken forward for further analysis if the Coronavirus pandemic had not occurred.

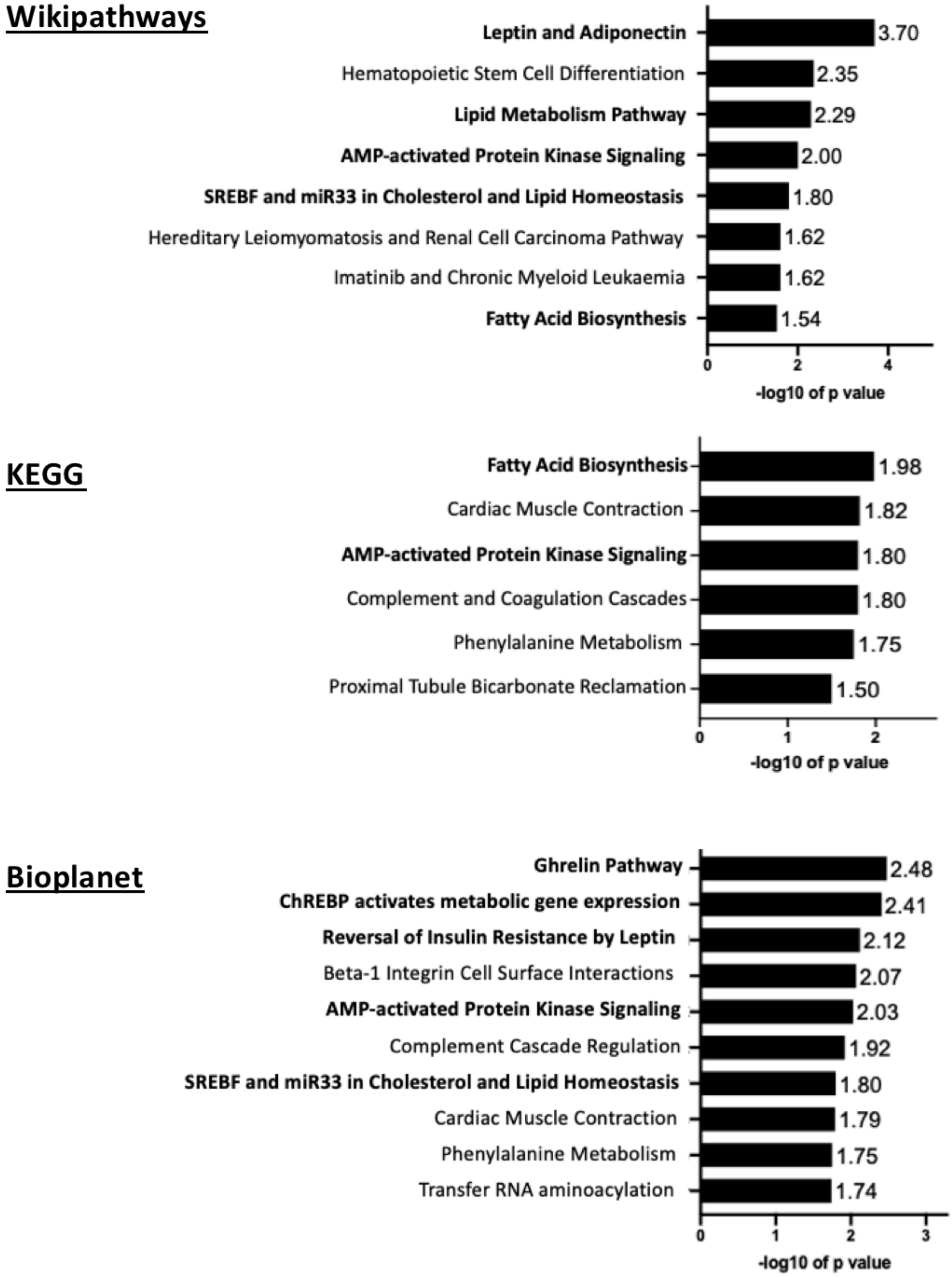

Figure 10: Gene ontology analysis of common gene targets for GR and LXRα. The list of 243 GR and LXRα coregulated genes from figure 9, were input into Enrichr, a platform which searches a panel of ontology databases to predict altered pathways based on gene signatures. Graph shows significantly enriched pathways from three databases; Wikipathways, KEGG and Bioplanet. Bold font indicates pathways related to lipid metabolism. -log10 p value is plotted in each case, so higher values denote increased significance.

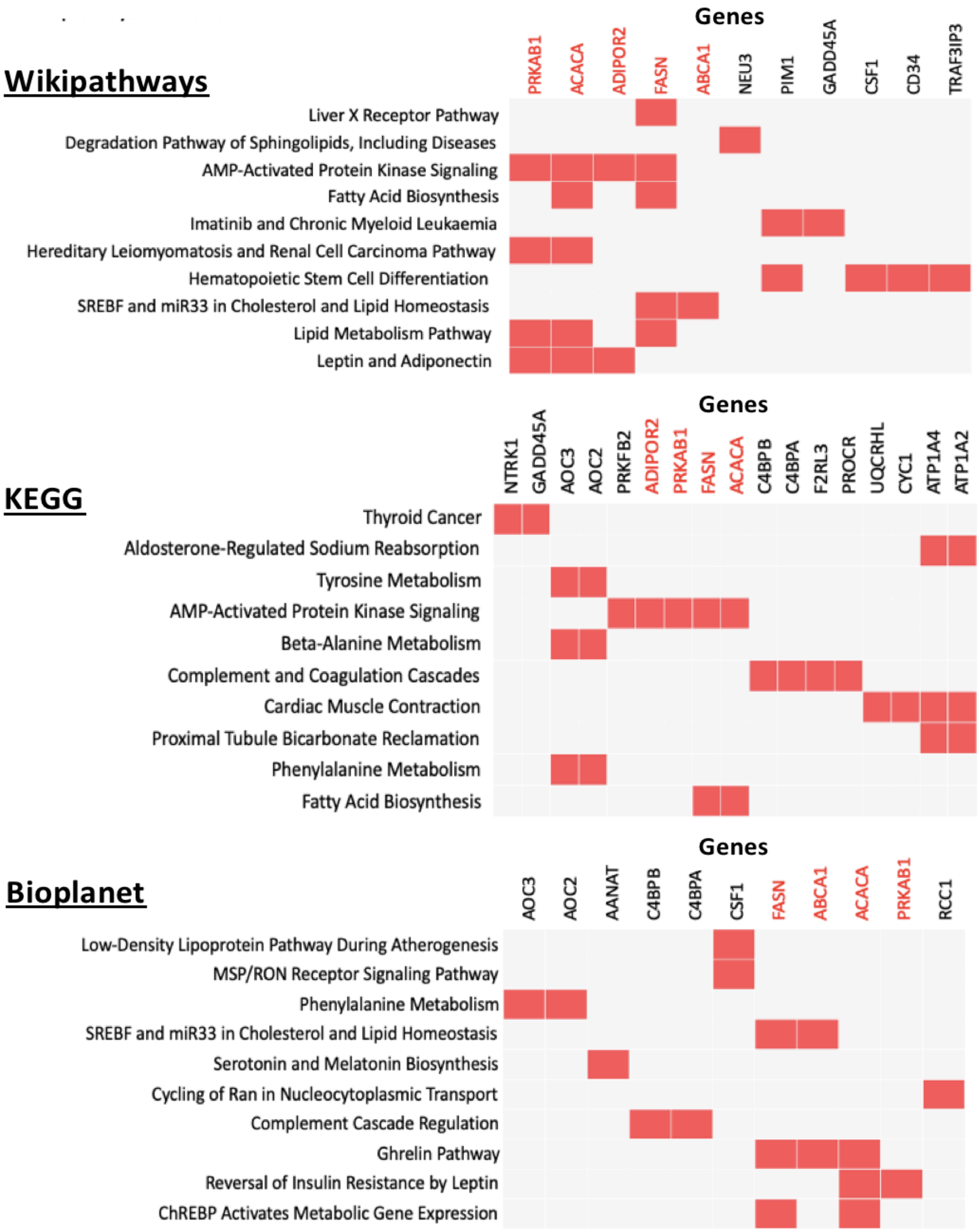

Figure 11: Clustergram analysis of the 243 GR and LXRα shared gene targets. The analysis from figure 10 was extended to visualise individual genes within the top 10 enriched pathways. Clustergrams shows significant regulation of genes that are enriched in the top 10 ontologies (red squares) from all three databases; Wikipathways, KEGG and Bioplanet. Red font indicates candidate genes that were highlighted by multiple independent databases.

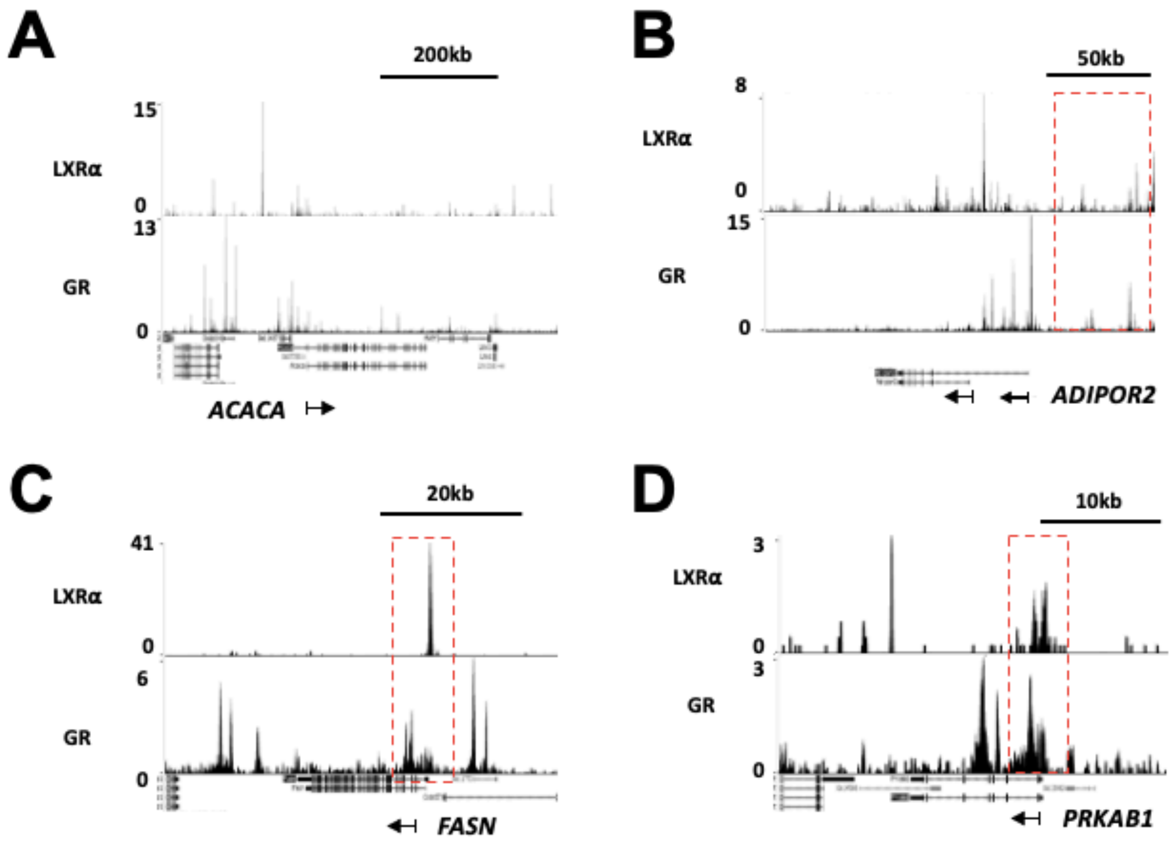

Figure 12: Mapping LXRα and GR, binding sites using data from the Cistrome database. Gene tracks for the three nuclear receptors were visualised in UCSC genome browser to identify common binding (peaks) at, or upstream of transcriptional start sites (28,31,32,36). The four candidate coregulated genes *ACACA, ADIPOR2, FASN* and *PRKAB1* are shown. Arrows below indicate transcriptional start site and direction of transcription. Red dashed boxes highlights potential regions for coregulation. Y-axis shows peak/ binding score. Scale in kilobases (Kb) shown for each gene.

Discussion

Due to the Coronavirus pandemic there was not time to complete sufficient biological replicates for the wet lab experiments. This was a frustration, as I had received training, and gained confidence in a variety of techniques but was unable to build on my experience. Consequently, no statistical analysis could be completed on the data and hence it is not possible to determine if any differences seen between treatments are due to random chance or biologically meaningful effects. Future work should complete experimental repeats to enable statistical analysis, complete PCR to confirm GR and LXR regulation of *ADIPOR2*, *FASN*, and *PRKAB1*, and complete LipidTox assays to define the effect of OCDO on lipid accumulation.

This study adds evidence that OCDO binds directly to GR and activates GR-mediated transcription. It also adds evidence that OCDO activates LXR-mediated transcription and identifies a point of crosstalk between GR and LXR relevant to metabolism.

A COVID-affected course experience

Despite lab work ending prematurely, during my six months in the lab I gained valuable experiences in the scientific techniques described above. I developed problem-solving skills from talking with my lab group to work out why a technique I had been trying for a number of weeks wasn't working (which taught me why research can take a long time!) to deciding the best datasets to use from the limited number available. Through these experiments and being part of weekly lab group meetings I gained an appreciation for the number of variable factors in an experiment, for example the antibody quality. I learnt how to critically appraise a paper during paper criticism tutorials and 1:1 conversations with my supervisors and I developed academic writing skills whilst writing my literature review and project report. Together these experiences helped me appreciate the level of rigor research requires to demonstrate a theory. Informal lab meetings and seminars were excellent opportunities to hear about other research projects and techniques as well as present my work too.

Whilst pre-COVID I was happy working quietly I found working from home during the lockdown period challenging, particularly when we could only exercise once a day, because it was harder to split the day into sections. However, the experience made me reflect on how I work best but also implement strategies to maintain productivity. Regular meetings with my supervisors were helpful for goal setting and kept the project progressing, plus, there was plenty of time for reading papers.

There are so many unanswered questions in pathology. I look forward to using the skills which I developed this year in the future to help improve our understanding of diseases and new ways of treating them.

Word count: 1,997 (excluding figure legends)

Acknowledgements

Thank you to my supervisors, Dr Laura Matthews and Dr James Thorne, for all of their support and advice throughout this project and for conceiving the project hypothesis. Pauline Pfaender completed the string network analysis which identified GR and LXR as part of an enriched metabolic signature in TNBC which provided the instruction for the project. Thank you to Freya Leif, Fiona Leslie, and Kathryn McGinnis for demonstrating the laboratory and analysis techniques to me.

Thank you to the Pathological Society and the Wolfson Foundation for their generous sponsorship of this project.

References

1. BreastCancerNow. Facts and statistics 2019. 2019.
2. Korourian S, Kumarapeli A, Klimberg V. The Breast Comprehensive Management of Benign and Malignant Diseases [Internet]. 5th ed. Bland K, Copeland E, Klimberg V, Gradishar W, editors. Philadelphia: Elesvier; 2018. 197–206 p. Available from: https://www.sciencedirect.com/book/9780323359559/the-breast#book-description
3. Santa-Maria, CA Gradishar W. Adjuvant and Neoadjuvant Systemic Therapies for Early-Stage Breast Cancer. In: Bland K, Copeland E, Klimberg V, Gradishar W, editors. The Breast: Comprehensive Management of Benign and Malignant Diseases [Internet]. 5th ed. Elesvier; 2018. p. 752–62. Available from: https://reader.elsevier.com/reader/sd/pii/B9780323359559000556?token=D5378ADE9C49B3FF4696935AF790E46E97003247C45690214761419B3DCC2746E680EDE8C92E31134858B855895D45F7
4. Beniey M, Haque T, Hassan S. Translating the role of PARP inhibitors in triple-negative breast cancer. Oncoscience [Internet]. 2019;6(1–2):287–8. Available from: https://www.ncbi.nlm.nih.gov/pmc/articles/PMC6382255/
5. NICE. Early and locally advanced breast cancer: diagnosis and management. 2018.
6. Cortazar P, Zhang L, Untch M, Mehta K, Costantino JP, Wolmark N, et al. Pathological complete response and long-term clinical benefit in breast cancer: The CTNeoBC pooled analysis. Lancet [Internet]. 2014;384(9938):164–72. Available from: https://pdf.sciencedirectassets.com/271074/1-s2.0-S0140673614X60927/1-s2.0-S0140673613624228/main.pdf?X-Amz-Security-Token=IQoJb3JpZ2luX2VjELf%2F%2F%2F%2F%2F%2F%2F%2F%2F%2FwEaCXVzLWVhc3QtMSJHMEUCIDWNCYO7OQX86u8OD2LfCeBkUge%2FQ38OmUaWxxJsf1gqAiEA4iuyRbFRSA
7. Huang W, Glass CK. Nuclear receptors and inflammation control: Molecular mechanisms and pathophysiological relevance. Arterioscler Thromb Vasc Biol. 2010;30(8):1542–9.
8. Sever R, Glass CK. Signaling by nuclear receptors. Cold Spring Harb Perspect Biol [Internet]. 2013;5(3):20894. Available from: https://www.ncbi.nlm.nih.gov/pmc/articles/PMC3578364/
9. Evans RM. The steroid and thyroid hormone receptor superfamily. Science

(80-) [Internet]. 1988;240(4854):889–95. Available from: https://www.ncbi.nlm.nih.gov/pmc/articles/PMC6159881/
10. Pratt W, Toft D. Steroid Receptor Interactions with Heat Shock Protein and Immunophilin Chaperones. Endocr Rev [Internet]. 1997 Jun 1;18(3):306–60. Available from: https://academic.oup.com/edrv/article/18/3/306/2530755
11. Skor MN, Wonder EL, Kocherginsky M, Goyal A, Hall BA, Cai Y, et al. Glucocorticoid receptor antagonism as a novel therapy for triple-negative breast cancer. Clin Cancer Res. 2013 Nov 15;19(22):6163–72.
12. Han H, Wilks S, Paplomata E, Modiano M, Becerra C, Braiteh F, et al. Abstract P6-12-15: Efficacy results of a phase 1/2 study of glucocorticoid receptor (GR) antagonist mifepristone (MIFE) in combination with eribulin in GR-positive triple-negative breast cancer (TNBC). In American Association for Cancer Research (AACR); 2017. p. P6-12-15-P6-12–5.
13. Nanda R, Stringer-Reasor EM, Saha P, Kocherginsky M, Gibson J, Libao B, et al. A randomized phase I trial of nanoparticle albumin-bound paclitaxel with or without mifepristone for advanced breast cancer. Springerplus [Internet]. 2016 Dec 1;5(1). Available from: https://springerplus.springeropen.com/track/pdf/10.1186/s40064-016-2457-1
14. Pratt WB, Toft DO. Steroid Receptor Interactions with Heat Shock Protein and Immunophilin Chaperones*. Endocr Rev [Internet]. 1997 Jun 1;18(3):306–60. Available from: https://academic.oup.com/edrv/article/18/3/306/2530755
15. Voisin M, De Medina P, Mallinger A, Dalenc F, Huc-Claustre E, Leignadier J, et al. Identification of a tumor-promoter cholesterol metabolite in human breast cancers acting through the glucocorticoid receptor. Proc Natl Acad Sci U S A. 2017 Oct 31;114(44):E9346–55.
16. Iñiguez-Lluhí JA, Lou DY, Yamamoto KR. Three Amino Acid Substitutions Selectively Disrupt the Activation but Not the Repression Function of the Glucocorticoid Receptor N Terminus. J Biol Chem. 1997;272(7):4149–56.
17. Lai SC, Phelps CA, Short AM, Dutta SM, Mu D. Thyroid transcription factor 1 enhances cellular statin sensitivity via perturbing cholesterol metabolism. Oncogene. 2018;
18. Mei S, Qin Q, Wu Q, Sun H, Zheng R, Zang C, et al. Cistrome Data Browser: A data portal for ChIP-Seq and chromatin accessibility data in human and mouse. Nucleic Acids Res. 2017;45(D1):D658–62.
19. Zheng R, Wan C, Mei S, Qin Q, Wu Q, Sun H, et al. Cistrome Data Browser: Expanded datasets and new tools for gene regulatory analysis. Nucleic Acids Res. 2019;47(D1):D729–35.
20. Enuka Y, Feldman ME, Chowdhury A, Srivastava S, Lindzen M, Sas-Chen A, et al. Epigenetic mechanisms underlie the crosstalk between growth factors and a steroid hormone. Nucleic Acids Res. 2017;45(22):12681–99.
21. Chen Z, Lan X, Wu D, Sunkel B, Ye Z, Huang J, et al. Ligand-dependent genomic function of glucocorticoid receptor in triple-negative breast cancer. Nat Commun. 2015;6.
22. Kolasinska-Zwierz P, Down T, Latorre I, Liu T, Liu XS, Ahringer J. Differential chromatin marking of introns and expressed exons by H3K36me3. Nat Genet. 2009;41(3):376–81.
23. Savic D, Ramaker RC, Roberts BS, Dean EC, Burwell TC, Meadows SK, et al. Distinct gene regulatory programs define the inhibitory effects of liver X receptors and PPARG on cancer cell proliferation. Genome Med. 2016;8(74).
24. Yan J, Enge M, Whitington T, Dave K, Liu J, Sur I, et al. Transcription Factor

Binding in Human Cells Occurs in Dense Clusters Formed Around Cohesin Anchor Sites. Cell [Internet]. 2013;514(4):801–13. Available from: https://pubmed.ncbi.nlm.nih.gov/23953112/
25. Pehkonen P, Welter-Stahl L, Diwo J, Ryynänen J, Wienecke-Baldacchino A, Heikkinen S, et al. Genome-wide landscape of liver X receptor chromatin binding and gene regulation in human macrophages. BMC Genomics. 2012;13(50).
26. Jing D, Bhadri VA, Beck D, Thoms JAI, Yakob NA, Wong JWH, et al. Opposing regulation of BIM and BCL2 controls glucocorticoid-induced apoptosis of pediatric acute lymphoblastic leukemia cells. Blood [Internet]. 2015;125(2):273–83. Available from: https://ashpublications.org/blood/article-lookup/doi/10.1182/blood-2014-05-576470
27. Galhardo M, Sinkkonen L, Berninger P, Lin J, Sauter T, Heinäniemi M. Integrated analysis of transcript-level regulation of metabolism reveals disease-relevant nodes of the human metabolic network. Nucleic Acids Res. 2014;42(3):1474–96.
28. Oishi Y, Spann NJ, Link VM, Muse ED, Strid T, Edillor C, et al. SREBP1 contributes to resolution of pro-inflammatory TLR4 signaling by reprogramming fatty acid metabolism. Cell Metab [Internet]. 2017;25(2):412–27. Available from: https://pubmed.ncbi.nlm.nih.gov/28041958/
29. Heinz S, Benner C, Spann N, Bertolino E, Lin YC, Laslo P, et al. Simple Combinations of Lineage-Determining Transcription Factors Prime cis-Regulatory Elements Required for Macrophage and B Cell Identities. Mol Cell. 2010;38(4):576–89.
30. Oh KS, Patel H, Gottschalk RA, Lee WS, Baek S, Fraser IDC, et al. Anti-Inflammatory Chromatinscape Suggests Alternative Mechanisms of Glucocorticoid Receptor Action. Immunity. 2017;47(2):298-309.e5.
31. Boergesen M, Pedersen TA, Gross B, van Heeringen SJ, Hagenbeek D, Bindesboll C, et al. Genome-Wide Profiling of Liver X Receptor, Retinoid X Receptor, and Peroxisome Proliferator-Activated Receptor in Mouse Liver Reveals Extensive Sharing of Binding Sites. Mol Cell Biol. 2012;32(4):852–67.
32. Grøntved L, John S, Baek S, Liu Y, Buckley JR, Vinson C, et al. C/EBP maintains chromatin accessibility in liver and facilitates glucocorticoid receptor recruitment to steroid response elements. EMBO J. 2013;32(11):1568–83.
33. Bioinformatics & Evolutionary Genomics. Biovenn [Internet]. [cited 2020 Jan 21]. Available from: http://bioinformatics.psb.ugent.be/webtools/Venn/
34. Chen EY, Tan CM, Kou Y, Duan Q, Wang Z, Meirelles G V., et al. Enrichr: Interactive and collaborative HTML5 gene list enrichment analysis tool. BMC Bioinformatics. 2013;14.
35. Kuleshov M V., Jones MR, Rouillard AD, Fernandez NF, Duan Q, Wang Z, et al. Enrichr: a comprehensive gene set enrichment analysis web server 2016 update. Nucleic Acids Res. 2016;44(W1):W90–7.
36. Tyner C, Barber GP, Casper J, Clawson H, Diekhans M, Eisenhart C, et al. The UCSC Genome Browser database: 2017 update. Nucleic Acids Res. 2017;45(D1):D626–34.

Appendix

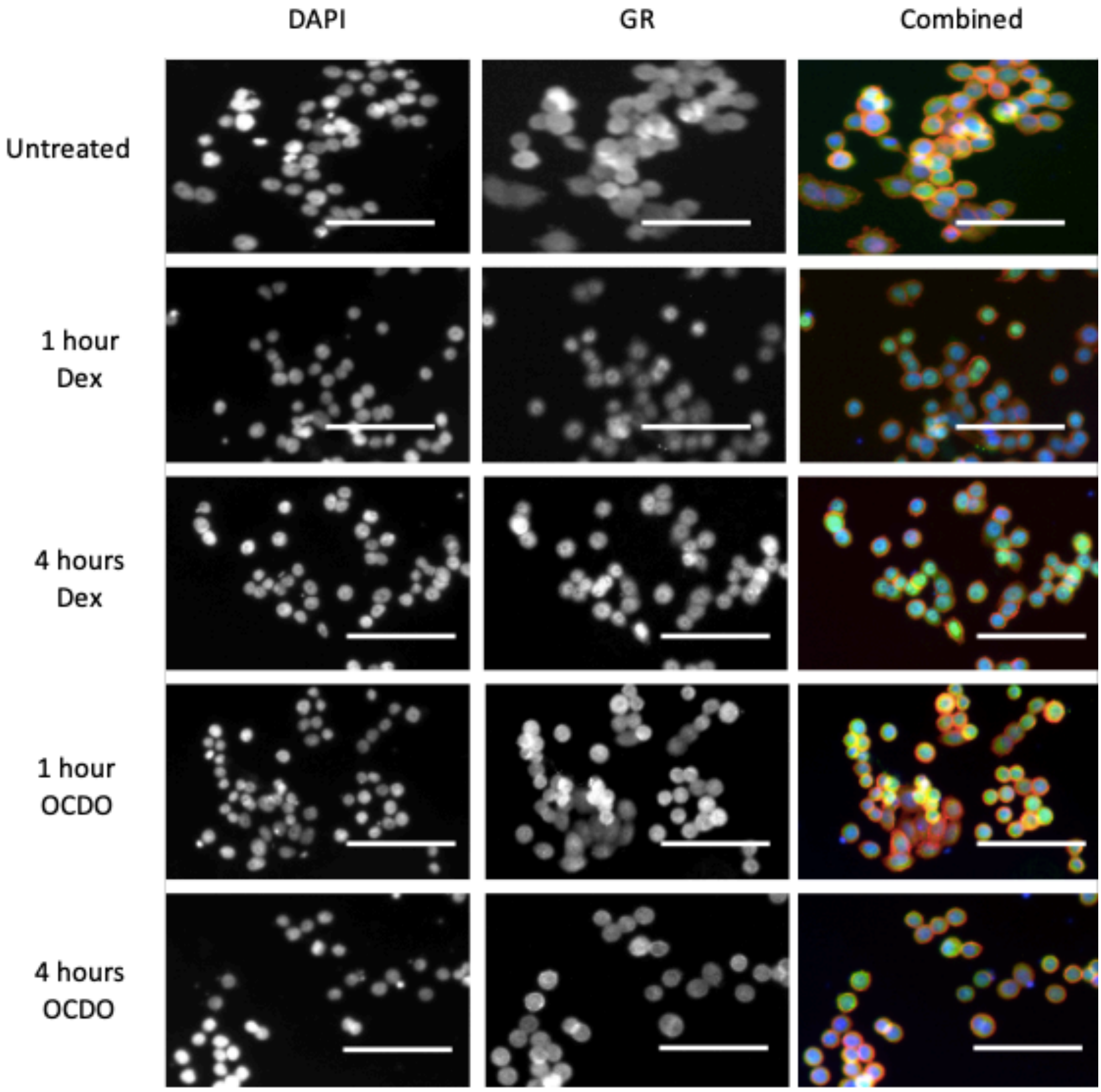

Figure A: Ligand induced GR translocation in MDA-MB-468 cells after 4 hours. Representative immunofluorescence images for MDA-MB-468 cells treated for one or four hours with 100nM Dexamethasone or 10μM OCDO, then fixed and stained for DNA, actin and GR. Left column: greyscale images of nuclei identified with DAPI staining. Middle column: greyscale image of location of GR. Right column: Colour images of three stains. Red indicates actin, blue indicates the nucleus and green indicates GR. Scale bars indicate 50μm, 20x magnification. N=1.

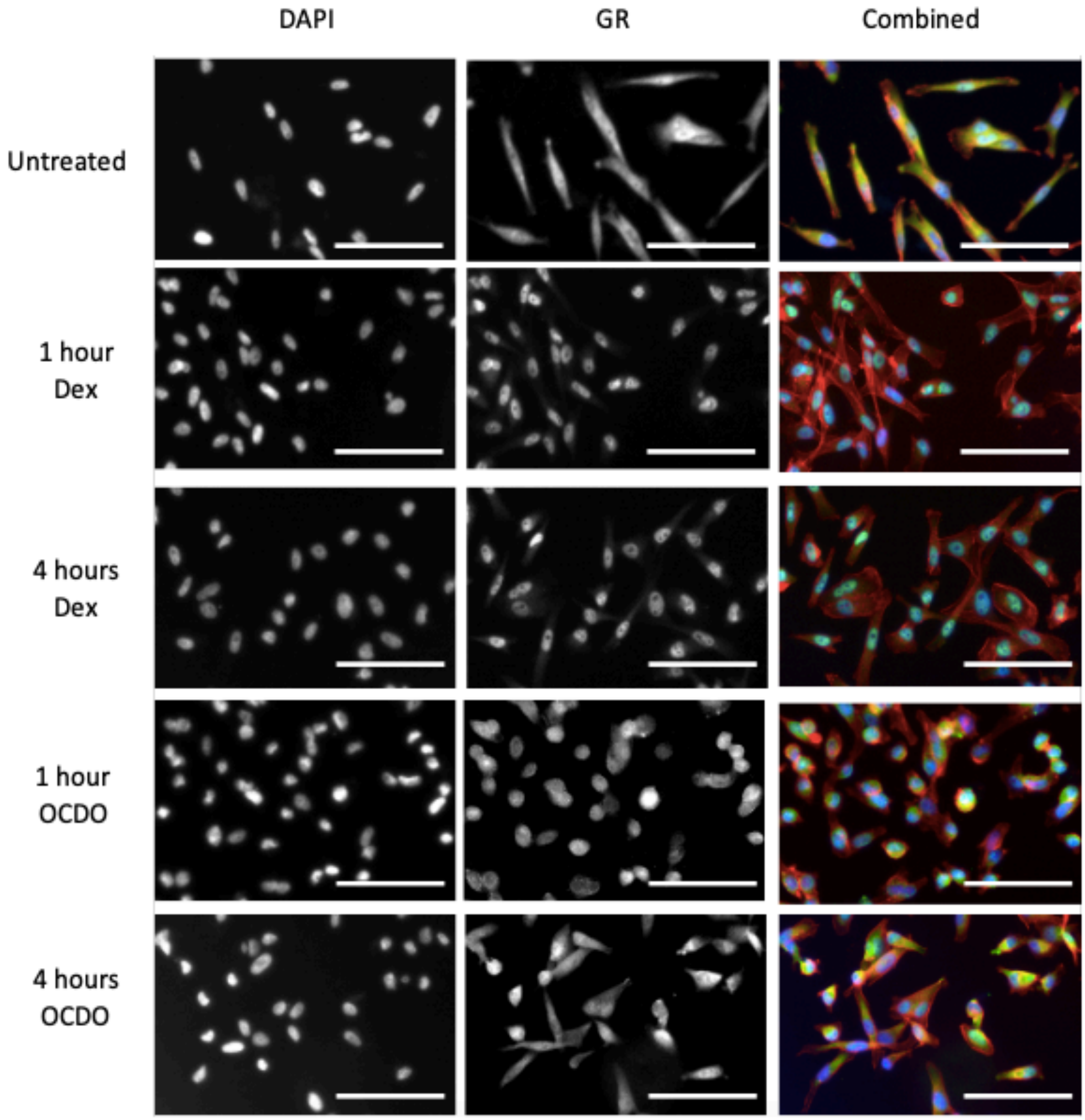

Figure B: Ligand induced GR translocation in MDA-MB-231 cells after 1 and 4 hours. Representative immunofluorescence images for MDA-MB-231 cells treated for one or four hours with 100nM Dexamethasone or 10μM OCDO, then fixed and stained for DNA, actin and GR. Left column: greyscale images of nuclei identified with DAPI staining. Middle column: greyscale image of location of GR. Right column: Colour images of three stains. Red indicates actin, blue indicates the nucleus and green indicates GR. Scale bars indicate 50μm, 20x magnification. N=1.

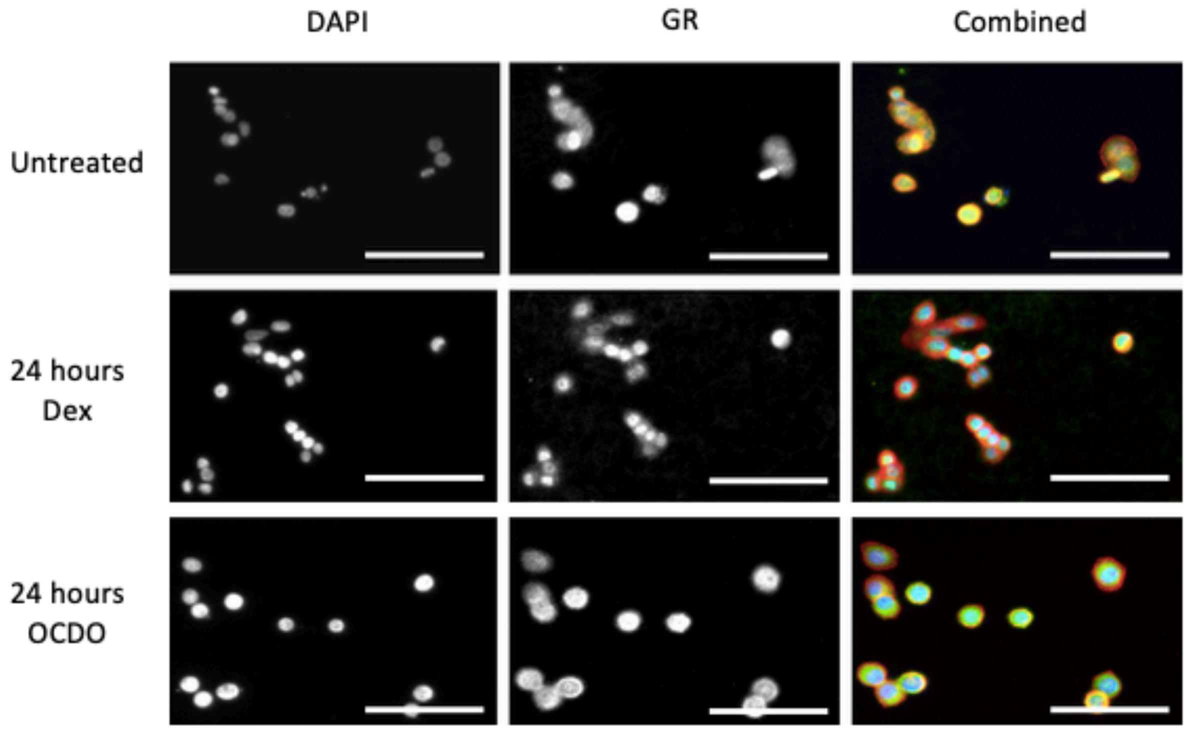

Figure C: Ligand induced GR translocation in MDA-MB-468 cells after 24hrs. Representative immunofluorescence images for MDA-MB-468 cells treated for 24 hours with 100nM Dexamethasone or 10µM OCDO, then fixed and stained for DNA, actin and GR. Left column: greyscale images of nuclei identified with DAPI staining. Middle column: greyscale image of location of GR. Right column: Colour images of three stains. Red indicates actin, blue indicates the nucleus and green indicates GR. Scale bars indicate 50µm, 20x magnification. N=1.

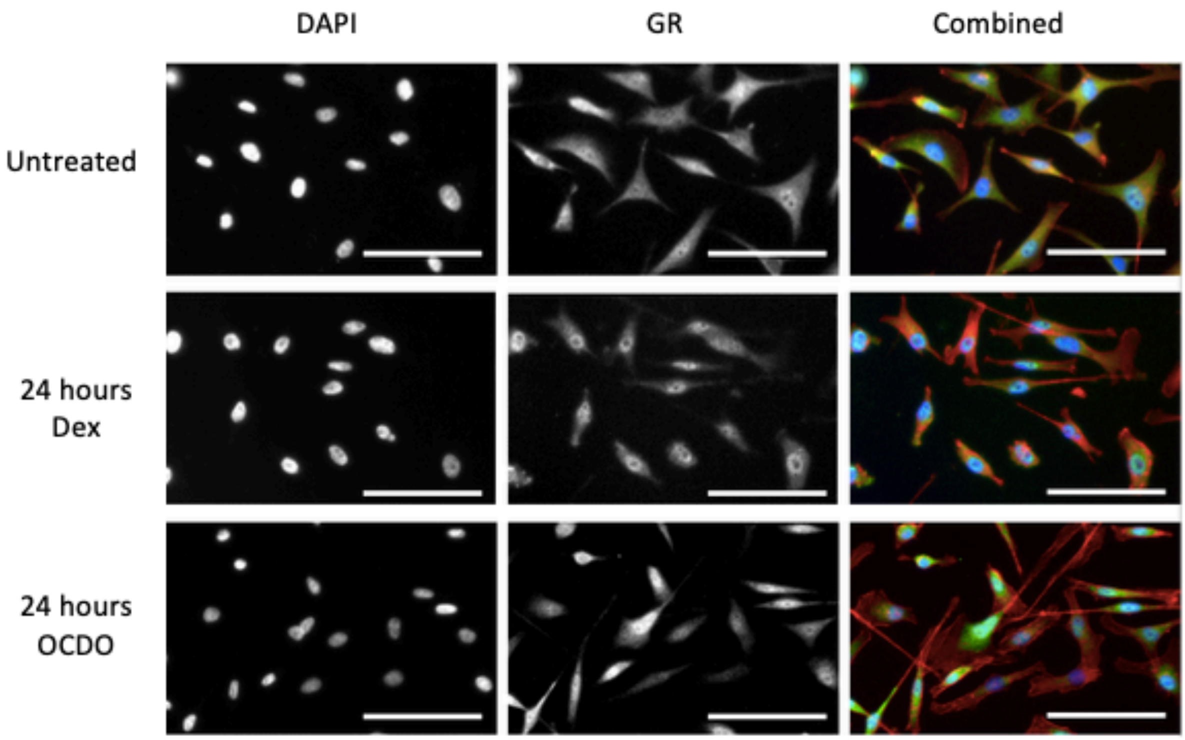

Figure D: Ligand induced GR translocation in MDA-MB-231 cells after 24hrs. Representative immunofluorescence images for MDA-MB-231 cells treated for 24 hours with 100nM Dexamethasone or 10µM OCDO, then fixed and stained for DNA, actin and GR. Left column: greyscale images of nuclei identified with DAPI staining. Middle column: greyscale image of location of GR. Right column: Colour images of three stains. Red indicates actin, blue indicates the nucleus and green indicates GR. Scale bars indicate 50µm, 20x magnification. N=1.